

Synthesis, Structure, and Dynamics of Tris(η^5 -cyclopentadienyl)lanthanides and Bis(η^5 -cyclopentadienyl)[bis(trimethylsilyl)amido]cerium(III)

Ulrich Baisch, Sandro Pagano, Martin Zeuner, Jörn Schmedt auf der Günne,
Oliver Oeckler, and Wolfgang Schnick*

Department Chemie und Biochemie, Ludwig-Maximilians-Universität München, Butenandtstrasse 5-13 (D),
D-81377 München, Germany

Received March 11, 2006

The crystal structures of tris(η^5 -cyclopentadienyl)lanthanides (Ln = Ce, Dy, Ho) have been determined using different X-ray diffraction methods. Cp₃Ce and Cp₃Ho (Cp = cyclopentadienyl) crystal data needed special solution and refinement methods, due to the occurrence of intrinsic twinning in these species. Our results do not agree with the previously published cell constants of Cp₃Ho. The space group and unit cell parameters of Cp₃Dy have been derived from powder diffraction experiments. High-resolution ¹³C solid-state NMR data of Cp₃La are presented, giving evidence of the dynamics and bonding situation of the Cp ligands. Cp₃Ce turned out to be a reactive reagent for the synthesis of bis(η^5 -cyclopentadienyl)-[bis(trimethylsilyl)amido]cerium(III).

Introduction

Homoleptic metal complexes represent convenient starting compounds for a wide range of synthetic approaches.^{1,2} Their crystal structure data are important references regarding bond distances and angles, physical properties, and chemical behavior for all kinds of heteroleptic successors.^{1–3} Synthesis and crystal structure solutions of base free homoleptic Cp complexes (Cp = cyclopentadienyl) are still a matter of recent research.^{4–8}

Cp₃Ln species (Ln = La–Lu) are essential starting compounds in organometallic rare-earth chemistry^{1–3,9–11} and have been known since the earliest days in lanthanide chemistry.^{11–13} It is remarkable that only 8 of the 15 possible Cp₃Ln (Ln = La–Lu) crystal structures have been reported as yet.³ Furthermore, no solid-state NMR studies concerning the ring dynamics are known.

Single crystals suitable for X-ray diffraction experiments are often very difficult to obtain, due to the fast crystallization of these homoleptic ionic complexes and the motion of the Cp ligands. We observed intrinsic twinning of Cp₃Ce, Cp₃Dy, and Cp₃Ho crystals. X-ray diffraction techniques at different temperatures have been elaborated to finally succeed in the first crystal structure determination of Cp₃Ho and Cp₃Ce and the determination of the cell parameters of crystalline Cp₃Dy. High-resolution NMR of Cp₃La has been carried out and turned out to be a powerful technique with respect to dynamics and the bonding situation of the controversially discussed solid-state structure of Cp₃La,^{14,15} which is a model compound for the whole Cp₃Ln series.

Furthermore, we report the synthesis of bis(η^5 -cyclopentadienyl)[bis(trimethylsilyl)amido]cerium(III) by the reaction of Cp₃Ce and [Ce{NSi(Me)₃}₂]₃. The reaction product shows a remarkable reactivity and represents a suitable reagent for further investigations in solid-state chemistry.

Results and Discussion

Diffraction Studies of Cp₃Ln (Ln = Ce, Dy, Ho). The solid-state structures of Cp₃Ln are reported to vary significantly along the Ln series. Table 1 shows the cell parameters of structure determinations reported in the literature.^{14–25}

It is remarkable that obtaining suitable single crystals of Cp₃Ln complexes in the central part of the Ln period has been a problem. No single-crystal structure determinations of these compounds have been published as yet. Cp₃Sm–Cp₃Gd were analyzed by Laubereau et al.²⁴ using single-crystal and powder diffraction measurements to determine the space group. The

* To whom correspondence should be addressed. Tel: +49/89-2180-77436. Fax: +49/89-2180-77440. E-mail: wolfgang.schnick@uni-muenchen.de.

(1) Anwander, R.; Herrmann, W. A.; Scherer, W.; Munck, F. C. *J. Organomet. Chem.* **1993**, *462*, 163.

(2) Edelmann, F. T. In *Synthetic Methods of Organometallic and Inorganic Chemistry*, 1st ed.; Herrmann, W. A., Brauer, G., Eds.; Georg Thieme: Stuttgart, New York, 1997; Vol. 6, p 88.

(3) Anwander, R.; Herrmann, W. A. *Top. Curr. Chem.* **1996**, *179*, 1.

(4) Dinnebier, R. E.; Behrens, U.; Olbrich, F. *Organometallics* **1997**, *16*, 3855.

(5) Dinnebier, R. E.; Olbrich, F.; Bendele, G. M. *Acta Crystallogr., Sect. C: Cryst. Struct. Commun.* **1997**, *C53*, 699.

(6) Dinnebier, R. E.; Olbrich, F.; van Smaalen, S.; Stephens, P. W. *Acta Crystallogr., Sect. B: Struct. Sci.* **1997**, *B53*, 153.

(7) Panda, T. K.; Gamer, M. T.; Roesky, P. W. *Organometallics* **2003**, *22*, 877.

(8) Weber, F.; Sitzmann, H.; Schultz, M.; Sofield, C. D.; Andersen, R. A. *Organometallics* **2002**, *21*, 3139.

(9) Baisch, U.; Pagano, S.; Zeuner, M.; Barros, N.; Maron, L.; Schnick, W. *Chem. Eur. J.* **2006**, *12*, in press.

(10) Schumann, H.; Messe-Marktscheffel, J. A.; Esser, L. *Chem. Rev.* **1995**, *95*, 865.

(11) Wilkinson, G.; Birmingham, J. M. *J. Am. Chem. Soc.* **1954**, *76*, 6210.

(12) Fischer, E. O.; Fischer, H. *J. Organomet. Chem.* **1966**, *6*, 141.

(13) Fischer, H. Ph.D. Thesis, Technische Hochschule München, München, Germany, 1965.

(14) Eggers, S. H.; Kopf, J.; Fischer, R. D. *Organometallics* **1986**, *5*, 383.

(15) Rebizant, J.; Apostolidis, C.; Spirlet, M. R.; Kanellakopulos, B. *Acta Crystallogr., Sect. C: Cryst. Struct. Commun.* **1988**, *44*, 614.

(16) Bel'skii, V. K.; Gun'ko, Y. K.; Soloveichik, G. L.; Bulychev, B. M. *Metalloorg. Khim.* **1991**, *4*, 577.

(17) Eggers, S. H.; Hinrichs, W.; Kopf, J.; Fischer, R. D.; Xing-Fu, L. Cambridge Crystallographic Data Center, private communication, 1992 (CCDC No. CYPESM02).

Table 1. Cell Parameters of Crystal Structure Determinations of Cp₃Ln^a

	Cp ₃ La ^{14,15}		Cp ₃ Pr ²⁵	Cp ₃ Nd ²¹	Cp ₃ Pm ²⁰	Cp ₃ Sm ^{16–18}		Cp ₃ Gd ²⁰	Cp ₃ Tb ²⁰	Cp ₃ Ho ¹⁹	Cp ₃ Er ²²	Cp ₃ Tm ²²	Cp ₃ Yb ²³	Cp ₃ Lu ²⁴	
	<i>P2</i> ₁	<i>P2</i> ₁ / <i>c</i>				<i>P2</i> ₁ / <i>n</i>	<i>Pbcm</i>								
space group	<i>P2</i> ₁	<i>P2</i> ₁ / <i>c</i>	<i>P2</i> ₁	<i>P2</i> ₁ 2 ₁ 2 ₁	<i>Pbc</i> *	<i>P2</i> ₁ / <i>n</i>	<i>Pbcm</i>	<i>Pbcm</i>	<i>Pbc</i> *	<i>Pbc</i> *	<i>Pbc</i> *	<i>Pna</i> 2 ₁	<i>Pna</i> 2 ₁	<i>P2</i> ₁ 2 ₁ 2 ₁	<i>Pbc</i> 2 ₁
<i>a</i> (pm)	8.43(1)	15.24(1)	8.31(1)	8.80(1)	14.12(7)	9.79(1)	8.77(1)	14.23(2)	14.09(7)	14.20(7)	14.02(8)	19.72(1)	19.99(1)	7.99(1)	13.18(1)
<i>b</i> (pm)	9.85(1)	9.79(1)	9.71(1)	12.21(1)	17.60(9)	16.42(1)	9.79(1)	17.40(1)	17.52(9)	17.28(9)	17.3(1)	13.89(1)	13.79(1)	8.31(1)	8.93(1)
<i>c</i> (pm)	8.46(1)	16.72(1)	8.37(1)	9.76(1)	9.76(5)	20.40(1)	14.17(1)	9.73(2)	9.65(5)	9.65(5)	9.65(6)	8.62(1)	8.57(1)	18.17(1)	9.95(1)
β (deg)	115.8(1)	93.9(1)	116.1(1)			79.2(1)									
<i>V</i> (10 ⁴ pm ³)	631(1)	2489(2)	607(1)	1220(1)	2425(1)	3221(1)	1217(1)	2409(1)	2382(1)	2368(1)	2340(1)	2363(1)	2366(1)	1206(1)	1171(1)

^a Cell parameters obtained from powder diffraction experiments are denoted with an asterisk. Data for all Cp₃Ln crystals reported were measured at room temperature.

complexes were all suggested to crystallize in an orthorhombic primitive lattice with the space group *Pbcm*. The crystal structures were found to be isotypic with a single-crystal determination of Cp₃Sm.²⁵ Haug²² reported powder diffraction studies of Cp₃Ho and suggested the same space group as already determined for the compounds mentioned by Laubereau et al.²⁴

Cp₃Ho. Our diffraction experiments did not confirm the crystal structure reported by Haug.²² Single-crystal measurements at room temperature as well as at 130 K resulted in different cell parameters for the room-temperature and the low-temperature studies. Orthorhombic symmetry was observed at the low-temperature measurement with *a* = 843.0(2) pm, *b* = 970.4(2) pm, *c* = 1408.5(3) pm, and *V* = 1152(1) 10⁶ pm³. The *b* axis was half as long as reported by Haug.²² During the refinement procedure the heavy-atom positions became stable whereas the carbon positions remained heavily unstable. Pseudo merohedral twinning was detected after a further, more detailed analysis of the reciprocal space.²⁶ The structure was then solved and could easily be refined in the monoclinic space group *P2*₁/*c*. Table 2, Table 3, and Figure 1 show the crystallographic data, bond lengths and angles, and the molecular structure of Cp₃Ho, respectively.

Two molecular units are situated in the asymmetric unit of the unit cell. Three Cp rings are η^5 bonded to the central atom and do not form a trigonal-planar environment. The metal ion is slightly shifted, and the three centroids (Ctr) of the Cp ligands are the edges of a very flat trigonal pyramid formed by the metal atom and the ligands (Figure 1).

The reason for this arrangement is an additional η^1 coordination of a carbon atom of a neighboring Cp₃Ho molecule. η^1 -C–Ho distances of 300 and 301.6 pm are observed. Due to the second interaction of the Cp2 and Cp6 ligands longer intramolecular distances of these ligands to the metal atom were observed (248.2, 245.9 pm). Therefore, a formal coordination number of CN = 10 was observed for the Ho^{III} ion. Figure 2 shows the unit cell of the structure (along cell axis *a*) and the intermolecular contacts of C21 and C63 with the metal center (dashed lines). A chainlike structure is formed along cell axis *c*.

The cell parameters for Cp₃Ho given in the literature are not in accordance with the results obtained by our X-ray diffraction

(18) Eggers, S. H.; Hinrichs, W.; Kopf, J.; Fischer, R. D.; Xing-Fu, L. Cambridge Crystallographic Data Center, private communication, 1992 (CCDC No. SOVYAD).

(19) Eggers, S. H.; Hinrichs, W.; Kopf, J.; Jahn, W.; Fischer, R. D. *J. Organomet. Chem.* **1986**, *311*, 313.

(20) Eggers, S. H.; Kopf, J.; Fischer, R. D. *Acta Crystallogr., Sect. C: Cryst. Struct. Commun.* **1987**, *43*, 2288.

(21) Eggers, S. H.; Schultze, H.; Kopf, J.; Fischer, R. D. *Angew. Chem., Int. Ed. Engl.* **1986**, *25*, 656; *Angew. Chem.* **1986**, *98*, 631.

(22) Haug, H. O. *J. Organomet. Chem.* **1971**, *30*, 53.

(23) Hinrichs, W.; Melzer, D.; Rehwoldt, M.; Jahn, W.; Fischer, R. D. *J. Organomet. Chem.* **1983**, *251*, 299.

(24) Laubereau, P. G.; Burns, J. H. *Inorg. Chem.* **1970**, *9*, 1091.

(25) Wong, C.-H.; Lee, T.-Y.; Lee, Y.-T. *Acta Crystallogr., Sect. B: Struct. Sci.* **1969**, *25*, 2580.

(26) Herbst-Irmer, R.; Sheldrick, G. M. *Acta Crystallogr., Sect. B: Struct. Sci.* **1998**, *54*, 443.

Table 2. Crystallographic Data for Cp₃Ho

formula	C ₁₅ H ₁₅ Ho
mol mass (g mol ⁻¹)	360.2
cryst syst	monoclinic
space group	<i>P2</i> ₁ / <i>c</i>
	pseudo-merohedral twinning
diffractometer device	Nonius Kappa CCD
cryst size (mm ³)	0.20 × 0.15 × 0.10
wavelength λ (pm)	71.073 (Mo K α)
temp <i>T</i> (K)	130
twin law	$\begin{pmatrix} 1 & 0 & 0 \\ 0 & -1 & 0 \\ 0 & 0 & -1 \end{pmatrix}$
twin ratio	0.6037(6)
lattice constants	
<i>a</i> (pm)	843.0(2)
<i>b</i> (pm)	1408.5(3)
<i>c</i> (pm)	1940.7(4)
β (deg)	90.02(3)
cell vol (10 ⁶ pm ³)	2304.4(8)
formula units/cell	8
ρ_{calcd} (g cm ⁻³)	2.076
μ (mm ⁻¹)	6.833
<i>F</i> (000)	1376
2 θ range (deg)	3.2–30.51
no. of measd rflns	22 295
no. of indep rflns	7025
no. of rflns with $F_o^2 \geq 2\sigma(F_o^2)$	6288
no. of refined params	290
max peak/min hole (e \AA^{-3})	2.060/−0.987
<i>R</i> _{int} / <i>R</i> _{σ}	0.0387/0.0406
<i>R</i> 1 ($I > 2\sigma(I)$)	0.0231
wR2	0.0415
GOF	1.028

Table 3. Selected Bond Distances (pm) and Angles (deg) of Cp₃Ho

Ho1–Ctr2	245.9(3)	Ho1–Ctr6	366.5(3)
Ho1–Ctr3	241.0(2)	Ho2–Ctr2	370.5(3)
Ho1–Ctr4	239.0(3)	Ho1–Ho2	571.7(2)
Ho2–Ctr1	241.2(2)	Ho1–Ho#2	579.3(2)
Ho2–Ctr5	239.2(2)	Ho2–C21	300.0(5)
Ho2–Ctr6	248.2(2)	Ho1–C63	301.6(4)
Ctr1–Ho2–Ctr5	119.02(1)	C21–Ho2–Ctr5	102.95(8)
Ctr1–Ho2–Ctr6	117.37(1)	C21–Ho2–Ctr6	94.57(7)
Ctr5–Ho2–Ctr6	117.85(1)	C63–Ho1–Ctr2	95.36(7)
Ctr2–Ho1–Ctr3	117.25(1)	C63–Ho1–Ctr3	97.96(6)
Ctr2–Ho1–Ctr4	118.67(1)	C63–Ho1–Ctr4	102.11(6)
Ctr3–Ho1–Ctr4	117.64(1)	Ho1–C21–Ho2	174.5(2)
C21–Ho2–Ctr1	96.46(8)	Ho1–C63–Ho2	170.0(2)

measurements (Table 2). Lattice constants of an orthorhombic unit cell were determined (Table 1). Different crystallization techniques have been undertaken, changing the sublimation temperature and pressure (10⁻¹–10⁻³ mbar, 170–250 °C) in order to crystallize a certain amount of crystalline material with the cell parameters given in the literature. Single crystals were also measured at room temperature in order to exclude the possibility of a phase transition at low temperatures. Furthermore, X-ray powder diffraction (XRD) experiments were carried

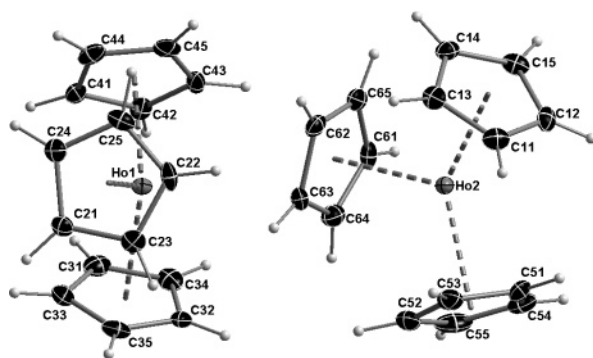


Figure 1. Asymmetric unit of the crystal structure of Cp_3Ho at 130 K (50% probability ellipsoids). The hydrogen atoms were calculated and refined using a riding model with fixed isotropic thermal parameters.

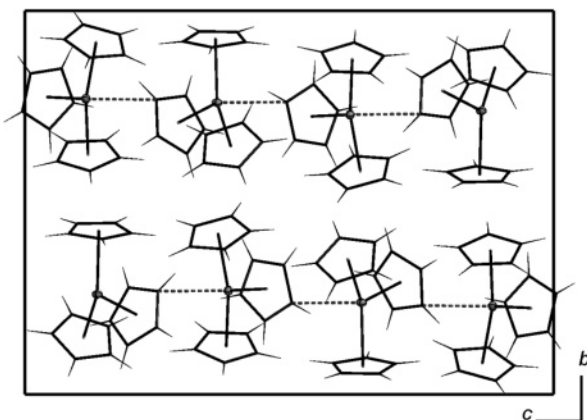


Figure 2. Projection of the unit cell of Cp_3Ho . View along axis a .

out at room temperature and low temperature. Phase transition was observed on cooling the crystalline material to 130 K; however, neither single-crystal nor powder diffraction measurements could confirm the cell parameters given in the literature (Table 1).

Cell parameters similar to those of Cp_3Ce (vide infra) were observed after both the refinement of the single-crystal data at room temperature and indexing of the powder patterns. A monoclinic primitive crystal system with $a = 1492.7(1)$ pm, $b = 964.0(1)$ pm, $c = 1629.8(1)$ pm, $\beta = 93.47(1)^\circ$, and $V = 2340.8(1) \times 10^6$ pm³ was determined. Reticular pseudo-merohedral twinning was detected for single crystals measured at room temperature. The separation of the twin domains and refinement of the structure were successfully carried out in space group $P2_1/c$. Figure 3 shows the similarity of the powder patterns obtained by our measurements and the results reported by Haug.²²

With a low 2θ resolution the most important structure-determining reflections (-102), (102) and (210), (-112) probably would not have been recognized and an orthorhombic cell would have been derived. In that case the (± 102) reflections (corresponding to (120) in $Pbcm$) would have shown the same 2θ position and the (210) reflection (corresponding to (201) in $Pbcm$) would have been systematically absent.

DyCp₃. Crystalline material was isolated by sublimation, and X-ray diffraction experiments showed even more complex diffraction patterns. The X-ray data collections of both powder and single-crystal material apparently gave strong evidence for an orthorhombic face-centered crystal system. None of them showed satisfying stability during the refinement process. Single-crystal measurements revealed intrinsic reticular pseudo-mero-

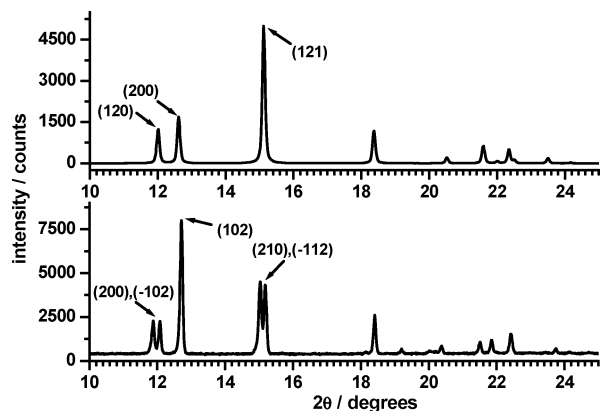


Figure 3. XRD patterns of Cp_3Ho ($\lambda_{\text{Cu K}\alpha} = 154.06$ pm). The orthorhombic cell calculated from literature data²² is depicted on the top. The monoclinic cell setting derived from the room-temperature measurement in our laboratory is depicted on the bottom.

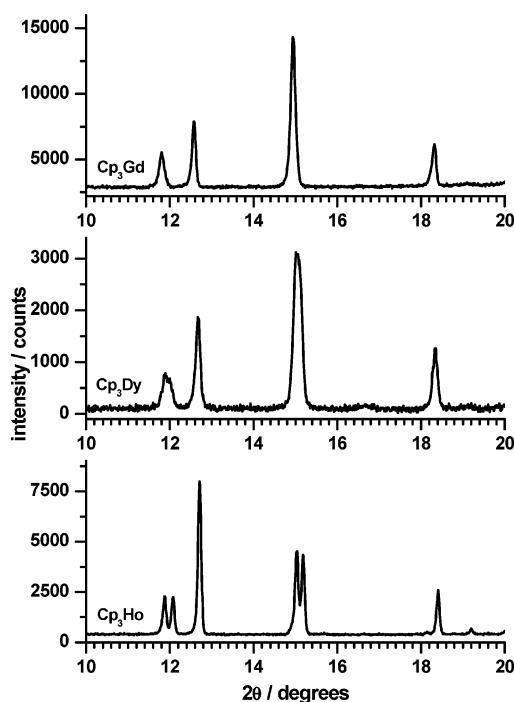


Figure 4. XRD patterns of Cp_3Ho , Cp_3Dy , and Cp_3Gd . Only the most relevant 2θ range is depicted ($\lambda_{\text{Cu K}\alpha} = 154.06$ pm).

hedral twinning, and additional disorder was detected. Incommensurate behavior is probable along cell axis c . Powder and single-crystal diffraction studies resulted in cell parameters of a monoclinic primitive crystal system with $a = 1642.0(3)$ pm, $b = 965.0(2)$ pm, $c = 1494.3(3)$ pm, $\beta = 93.94(2)^\circ$, and $V = 2362.2(2) \times 10^6$ pm³. Systematically absent reflections were indicating the space group $P2_1/c$.

These cell dimensions show similarity with the Cp_3Ho lattice constants (vide supra). In Figure 4 the most relevant 2θ ranges of experimental data for Cp_3Gd , Cp_3Dy , and Cp_3Ho are depicted. Whereas the (± 102) and (210), (-112) reflections are clearly separated in Cp_3Ho , the existence of two different reflections in Cp_3Dy can only be guessed by the broadened profiles in the pattern. In contrast to Cp_3Dy , the Cp_3Gd diagram shows more homogeneous reflection profiles and the orthorhombic cell parameters in the literature fit well with the experimental data.

Cp₃Ce. Cp_3Ce is the first homoleptic lanthanide metallocene in the series. It can be considered as the most reactive tris-

Table 4. Crystallographic Data for One Twin Domain of Cp₃Ce with and without Including the Overlapping Reflections into the Refinement Process

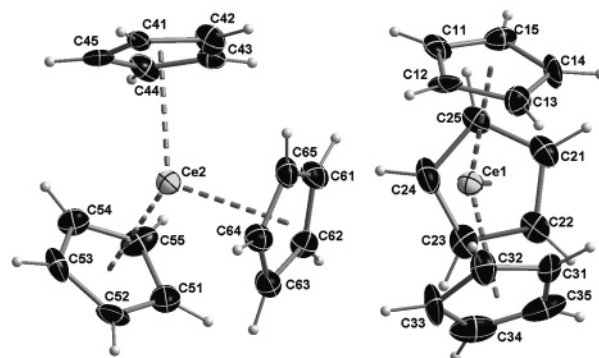
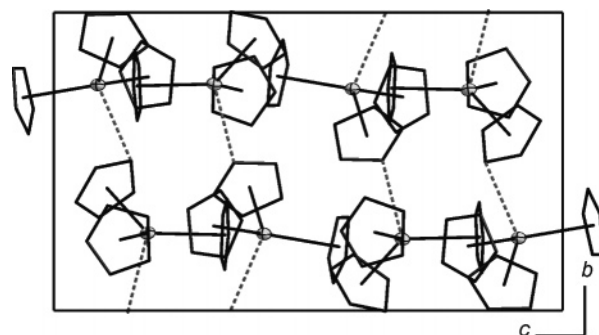
formula	C ₁₅ H ₁₅ Ce	
mol mass (g mol ⁻¹)	335.39	
cryst syst	monoclinic	
space group	P2 ₁ /c	
	reticular	
	pseudo-merohedral twinning	
diffractometer device	STOE IPDS	
cryst size (mm ³)	0.17 × 0.10 × 0.09	
wavelength λ (pm)	71.073 (Mo Kα)	
temp T (K)	100	
twin law		
	$\begin{pmatrix} 0.487 & 0 & -0.775 \\ 0 & -1 & 0 \\ -0.985 & 0 & -0.487 \end{pmatrix}$	
twin ratio	0.169(4)	
lattice constants		
<i>a</i> (pm)	1501.6(3)	
<i>b</i> (pm)	966.8(2)	
<i>c</i> (pm)	1662.1(3)	
β (deg)	93.10(3)	
cell vol (10 ⁶ pm ³)	2423.0(8)	
formula units/cell	8	
ρ _{calcd} (g cm ⁻³)	1.840	
μ (mm ⁻¹)	3.727	
<i>F</i> (000)	1304	
2θ range (deg)	2.76–25.30	
no. of mesh rflns	17 842	9921
no. of indep rflns	5338 for one individual	3249
no. of rflns with <i>F</i> _o ² ≥ 2σ(<i>F</i> _o ²)	9548	1964
no. of refined params	266	319
max peak/min hole (e Å ⁻³)	6.271/−2.676	1.432/−1.328
<i>R</i> _{int} / <i>R</i> _σ	0.1681/0.0767	0.1075/0.0907
<i>R</i> 1 (<i>I</i> > 2σ(<i>I</i>))	0.1069	0.0740
wR2	0.3180	0.1871
GOF	1.039	1.064

Table 5. Selected Bond Distances (pm) and Angles (deg) of Cp₃Ce

Ce1–Ctr1	251.2(6)	Ce1–Ctr6	359.4(6)
Ce1–Ctr2	253.1(6)	Ce2–Ctr2	352.7(6)
Ce1–Ctr3	259.6(6)	Ce1–Ce2	577.8(1)
Ce2–Ctr4	257.3(6)	Ce1–Ce#2	573.5(1)
Ce2–Ctr5	254.0(5)	Ce2–C21	295.5(12)
Ce2–Ctr6	251.4(6)	Ce1–C61	296.2(14)
Ctr1–Ce1–Ctr2	116.1(1)	C21–Ce2–Ctr5	107.9(1)
Ctr1–Ce1–Ctr3	117.4(1)	C21–Ce2–Ctr6	96.4(1)
Ctr2–Ce1–Ctr3	118.1(1)	C61–Ce1–Ctr1	97.9(1)
Ctr4–Ce2–Ctr5	117.6(1)	C61–Ce1–Ctr2	94.0(1)
Ctr4–Ce2–Ctr6	114.9(1)	C61–Ce1–Ctr3	106.8(1)
Ctr5–Ce2–Ctr6	116.7(1)	Ce1–C21–Ce2	172.13(1)
C21–Ce2–Ctr4	98.5(1)	Ce1–C51–Ce2	167.09(1)

(cyclopentadienyl)lanthanide.^{1,2} This strong Lewis acid reacts instantaneously with all kinds of electron-donating reagents. Due to this sensitivity Cp₃Ce would be appropriate for a variety of interesting and applicative reactions. On the other side this ability causes difficulties in crystallizing and isolating suitable crystals for X-ray diffraction experiments.

We did succeed in measuring data of a variety of crystals obtained by different sublimation conditions. None of these could be identified as real “single” crystals. Intrinsic reticular pseudo-merohedral multiple twinning was observed.²⁶ The best crystal isolated was used, and three data sets were extracted from the diffraction data. Cp₃Ce showed similar pseudo-orthorhombic symmetry as observed for Cp₃Ho and Cp₃Dy (vide supra), but X-ray powder diffraction experiments (XRD) confirmed a monoclinic cell setting. The reflections were

**Figure 5.** Asymmetric unit of the crystal structure of Cp₃Ce at 100 K (50% probability ellipsoids). The hydrogen atoms were calculated and refined using a riding model with fixed isotropic thermal parameters.**Figure 6.** Projection of the unit cell of Cp₃Ce along the unique axis *a*.

isolated, unifying all of the overlapping reflections of the three domains to one reflection set of the most appropriate individual. Subsequent determination of the twin law and refinement of the data resulted in a satisfying crystal structure refinement, taking into account the problems encountered during the isolation and weighting of the overlapping reflections in the reciprocal space. Table 4, Table 5, and Figure 5 show the crystallographic data, bond lengths and angles, and the molecular structure of Cp₃Ce, respectively.

The structure of Cp₃Ce is very similar to that of Cp₃Ho described above. Two molecular units are situated in the asymmetric unit of the unit cell. Three Cp rings are η⁵ bonded at the central atom, and the metal ion is slightly shifted from the theoretical center of gravity built by the three centroids (Ctr) of the Cp ligands. Additional intermolecular η¹ coordination of one carbon atom of a neighboring Cp₃Ce molecule is present as well. η¹-C–Ce distances of 295.5 and 296.2 pm have been measured, and a coordination number of CN = 10 is given for the Ce^{III} ion as well.

In this context the discrepancy between two structural studies of Cp₃La should be mentioned. According to Eggers et al.¹⁴ an additional intermolecular η² contact to the central atom does occur (*d*_{Ln–C} = 303.4 pm), whereas Rebizant et al.¹⁵ presumes only one additional η¹ contact due to the large second Ln–C distance (*d*_{Ln–C} = 332.9 pm). In Cp₃Ce the second nearest carbon atoms are C22 and C62 with distances of 333.4 and 343.5 pm, respectively. There is a difference of more than 40 pm to the next carbon atom. Thus, a second intermolecular contact cannot be observed in the solid-state structure of Cp₃Ce. Figure 6 shows the unit cell of the structure (along cell axis *a*) and the intermolecular contacts of C21 and C61 with the metal center (dashed lines). In comparison to the Cp₃Ho structure, a more zigzag-like arrangement of the complex molecules is observed.

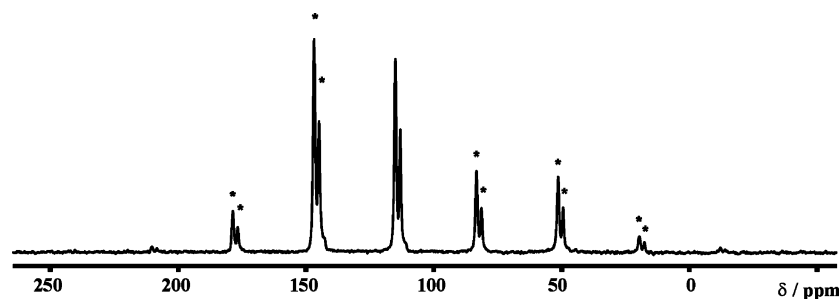


Figure 7. $^{13}\text{C}\{^1\text{H}\}$ CP MAS NMR spectrum of Cp_3La . Rotational sidebands of the isotropic chemical shifts δ_{iso} are marked by asterisks.

MAS NMR of Cp_3La . Ln^{III} complexes can be considered as a difficult species for solid-state NMR studies, because the majority of the compounds exhibit unpaired electrons. The corresponding lanthanum complex is an alternative with interesting properties close to those of the f-block elements, due to a small nuclear quadrupole moment ($Q = +0.20$ barn²⁷) of the abundant isotope ^{139}La . Additionally, no unpaired electrons are present in the complex.

Solid-state MAS NMR experiments²⁸ have been carried out for Cp_3La , in order to obtain additional information about the dynamic behavior of Cp ligands. This complex is discussed controversially in the literature regarding its crystal structure and the intermolecular interactions of the Cp ligands (vide infra). With respect to these, ^{13}C and ^1H measurements are promising probes.

^{13}C CP MAS NMR experiments showed the occurrence of only two sharp peaks in the spectrum (Figure 7). Normally one signal for each carbon atom would be expected, due to the low symmetry of the complex in the solid-state structure.

This discrepancy in the number of the observed signals is typical for metallocenes.^{29,30} The ^{13}C resonances of a single Cp anion are averaged by the ring dynamics being fast on the NMR time scale. Therefore, only a single resonance per ring can be observed. In the ^1H NMR spectrum one isotropic chemical shift at 6.3 ppm occurs, which agrees with liquid-state NMR data (6.0–6.3 ppm).² The low resolution of the signal is typical for single-pulse ^1H NMR.

Two well-resolved signals can be identified in the ^{13}C RAMP CP MAS NMR spectrum (Figure 7) at 115.0 and 113.1 ppm. The peak intensities show a ratio of 2:1. It can be interpreted as two Cp rings with similar distortion of the ideal gas-phase symmetry and one Cp ligand showing another signal caused by a larger distortion.

The observed spinning sidebands manifolds for each of the two signals are indicative of carbon chemical shift anisotropies in aromatic Cp systems and may be used as a spectroscopic fingerprint.^{29,30} Thus, sensitive parameters for symmetry and identity of the Cp ligands are the anisotropic chemical shift value δ_{aniso} and the asymmetry parameter η . The more intense and the less intense spinning sideband manifolds δ_{iso} 115.0, 113.1 are described by $\delta_{\text{aniso}} = -93.5(2)$, $-93.2(2.0)$ ppm and $\eta = 0.07(10)$, $0.29(5)$, respectively. The discrepancy between the two η values in the ^{13}C NMR experiment is consistent with the differences in distortion from an axial symmetry of the two types of Cp rings. The greater the η value, the more a distortion from the principal axial symmetry would occur. This is a strong

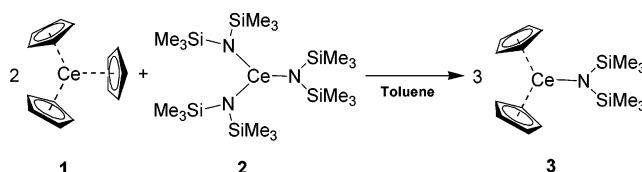
(27) Willans, M. J.; Feindel, K. W.; Ooms, K. J.; Wasylishen, R. E. *Chem. Eur. J.* **2005**, *12*, 159.

(28) Metz, G.; Wu, X.; Smith, S. O. *J. Magn. Reson. A* **1994**, *110*, 219.

(29) Hung, I.; Macdonald, C. L. B.; Schurko, R. W. *Chem. Eur. J.* **2004**, *10*, 5923.

(30) Hung, I.; Schurko, R. W. *Solid State Nucl. Magn. Reson.* **2003**, *24*, 78.

Scheme 1



indication for different coordination conditions for the Cp rings, where one ring with an additional η^1 coordination can be attributed to the signal with the weaker intensity (vide infra; Figures 2 and 6).

[$\text{Cp}_2\text{CeN}(\text{SiMe}_3)_2$]. The synthesis of Cp_2LnX systems has been studied extensively in the literature, but the formation of these compounds is often limited to the later lanthanide ions.^{1,3,9,12,14} Due to their smaller ionic radii these complexes are rather coordinatively saturated in comparison to the lighter lanthanides La, Ce, and Pr. As a matter of fact, more bulky ligands are generally reported for these complexes. Therefore, the synthesis of Cp^*CeX systems ($\text{Cp}^* =$ pentamethylcyclopentadienyl) is often described to be successful, in contrast to Cp_2CeX .^{31–36}

We successfully prepared bis(η^5 -cyclopentadienyl)[bis(tri-methylsilyl)amido]cerium(III) (**3**) by the reaction of Cp_3Ce (**1**) and $[\text{Ce}\{\text{N}(\text{SiMe}_3)_2\}_3]$ (**2**) in toluene (Scheme 1).

This reaction is very convenient, as apart from **1** and **2** there are no byproducts formed during the process. Therefore, it is better to use sublimed, solvent-free reagents. **1** shows only weak solubility in toluene at room temperature. To guarantee a proper formation of the product, the use of higher temperatures favors the reaction process. A yellow-orange mixture is obtained, and after evaporation of toluene the formation of an orange-yellow solid is observed. The orange product can be isolated easily by sublimation at 90 °C under vacuum (10^{-3} mbar). **3** shows weak red fluorescence on exposure to UV light ($\lambda = 366$ nm) and is very sensitive to air and moisture. The compound blackens immediately even by traces of oxygen.

3 was characterized by elemental analysis, IR, and MS experiments. IR experiments revealed both the typical stretching (ν_{CH} , ν_{CC}) and deformation vibrations (δ_{CH} (parallel), δ_{CH} (perpendicular)) for the cyclopentadienyl rings³⁷ at 3081, 1437, 1356, 1011, and 767 cm^{-1} and the typical stretching (ν_{CH} , ν_{SiC} ,

(31) Booij, M.; Kiers, N. H.; Heeres, H. J.; Teuben, J. H. *J. Organomet. Chem.* **1989**, *364*, 79.

(32) Evans, W. J.; Keyer, R. A.; Ziller, J. W. *Organometallics* **1993**, *12*, 2618.

(33) Heeres, H. J.; Renkema, J.; Booij, M.; Meetsma, A.; Teuben, J. H. *Organometallics* **1988**, *7*, 2495.

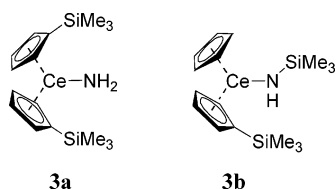
(34) Evans, W. J.; Perotti, J. M.; Kozimor, S. A.; Champagne, T. M.; Davis, B. L.; Nyce, G. W.; Fujimoto, C. H.; Clark, R. D.; Johnston, M. A.; Ziller, J. W. *Organometallics* **2005**, *24*, 3916.

(35) Clark, D. L.; Gordon, J. C.; Hay, P. J.; Poli, R. *Organometallics* **2005**, *24*, 5747.

(36) Li, Y.; Marks, T. J. *J. Am. Chem. Soc.* **1996**, *118*, 707.

(37) Fritz, H. P. *Adv. Organomet. Chem.* **1964**, *1*, 239.

Chart 1



ν_{SiN}) and deformation modes (δ_{Me} , δ_{SiC} , δ_{SiN}) for bis(trimethylsilyl)amido ligands² (BTSA ligands) at 2952, 1248, 1033, 839, 810, and 594 cm^{-1} . The IR signals are slightly shifted in comparison with those of the reagents. It was observed that Cp ligand vibrational modes are shifted versus higher wavenumbers, whereas signals attributed to the BTSA ligand did show wavenumbers slightly lower than those of the homoleptic BTSA complex. Cp ligands seem to be more strongly bonded to the metal center than in Cp_3Ce . Due to the higher electronic saturation of the central ion by the π -donating Cp ligands the BTSA group seems to be less bonded now. This is reasonable, because due to the reduced steric hindrance of a third Cp ligand the other ring ligands can coordinate nearer to the central metal, while the BTSA ligand, due to the steric hindrance of the SiMe_3 moiety, shows lower energetic vibrations compared to those of the homoleptic complex.

MS measurements carried out separately from the IR experiments showed a fragmentation pattern typical for **1** and **2**.³⁸ An M^+ peak could not be found in the mass spectrum; one hydrogen atom is abstracted instantaneously during the ionization process. The patterns of the molecule fragments of **3** showed the typical isotope manifolds expected for cerium complexes at m/z 429 ($\text{M} - \text{H}$), 358 ($\text{Cp}_2\text{CeNH}(\text{SiMe}_3)$), 344 ($\text{Cp}_2\text{CeNH}(\text{SiMe}_2)$), 293 ($\text{CpCeNH}(\text{SiMe}_3)$), and 269 (Cp_2Ce), proving the existence of the complex molecule. Reports have been found that silylated Cp ligands were formed during the reaction with silylamido derivatives.^{39,40} Thus, also other constitutions with the same molecular sum of 430 g/mol could be conceivable. Silylation of the Cp rings could occur in order to form (trimethylsilyl)-amino or nonsilylated compounds (**3a,b**), as depicted in Chart 1.

In comparison to a complex with only nitrogen-bonded SiMe_3 groups, Cp-bonded SiMe_3 groups show additional absorption signals (ν_{SiC} , δ_{SiC}) at lower wavenumbers in the regions 1300–1200 and 600–900 cm^{-1} . Vibrational modes in addition to those of **2** were not observed in the spectrum. The doubly N-silylated species **3** is the most plausible constitution for this compound, and the formation of **3a,b** can be considered as rather improbable.

Conclusion

Twinned crystals of Cp_3Ce , Cp_3Ho , and Cp_3Dy have been investigated by X-ray diffraction experiments and were all showing pseudo-orthorhombic symmetry during the determination of the solid-state structure. These difficulties are mainly caused by the formation of chainlike structures along one direction and the highly dynamic behavior of the Cp ligands in the solid state, even at low temperatures.

Whereas these problems are intrinsic for such systems in X-ray diffraction studies, due to the very short time scale during the measurement (occurrence of twinning, disorder, etc.), high-resolution MAS NMR studies of Cp_3La showed the existence

of two different bonding situations of the Cp ligands very well. These results can be considered as the first non-X-ray diffractive proof for chemical anisotropy in crystalline homoleptic lanthanide Cp complexes.

The synthesis of $[\text{Cp}_2\text{CeN}(\text{SiMe}_3)_2]$ (**3**) by the reaction of Cp_3Ce (**1**) and $[\text{Ce}\{\text{N}(\text{SiMe}_3)_2\}_3]$ (**2**) was reported. The reaction product was analyzed by IR/Raman spectroscopy, elemental analysis, and mass spectrometry. Nevertheless, a silylation of the Cp ring resulting in a mixture of isomers of different constitutions is possible. Endeavors to get suitable crystals for X-ray diffraction methods are in progress and will show which kind of molecule has mainly been formed in the solid state. In any event, **3** is an interesting agent, as this substance offers both high reactivity toward all kinds of electron-donating agents and sufficient thermal stability for solid-state reactions.

Experimental Section

General Procedures. All manipulations described below were performed with rigorous exclusion of oxygen and moisture in flame-dried Schlenk-type glassware on a Schlenk line, interfaced to a vacuum (10^{-3} mbar) line, or in an argon-filled glovebox. Argon was purified by passage over columns of silica gel, molecular sieve, KOH, P_2O_{10} , and titanium sponge (650 °C) and nitrogen by passage over columns of silica gel, molecular sieve, KOH, P_4O_{10} , BTS,⁴¹ and Cr^{II} oxide catalyst.⁴² Tetrahydrofuran (THF) was predried over KOH and distilled under argon over NaK alloy (benzophenone as indicator), and toluene was dried over LiAlH_4 pellets before distillation. Anhydrous lanthanide(III) chlorides were purchased from Alfa Aesar (99.99%, ultra dry) and were used without any further purification. LnCp_3 compounds ($\text{Ln} = \text{La}, \text{Ce}, \text{Dy}, \text{Ho}$) and $[\text{Ce}\{\text{N}(\text{SiMe}_3)_2\}_3]$ were prepared according to well-known procedures² and sublimed twice before use (10^{-3} mbar, 120–250 °C).

FTIR and FT Raman spectra were recorded with a Bruker IFS 66v/S spectrometer with DTGS detector. The samples were thoroughly mixed with dried KBr. The preparation procedures were performed in a glovebox under a dried argon atmosphere. The spectra were collected in a range from 400 to 4000 cm^{-1} with a resolution of 2 cm^{-1} . During the measurement, the sample chamber was evacuated. For FT Raman measurements, a Bruker FRA 106/S Raman module with a Nd:YAG laser (λ 1064 nm) and a scanning range from 0 to 3500 cm^{-1} was used. Mass spectra were measured with a JEOL MStation JMS700. The source was operated at different temperatures up to 100 °C. The powder diffraction investigations were carried out in Debye–Scherrer geometry, and diffraction data were collected on a conventional powder diffractometer (STOE Stadi P, Mo and Cu $\text{K}\alpha_1$ radiation). Products were identified using the STOE WinXPOW program package (Version 1.22, 1999).

$[\text{Cp}_2\text{CeN}(\text{SiMe}_3)_2]$. Two equivalents of **1** (0.66 mmol, 0.224 g) was suspended in a 100 mL Schlenk tube and stirred in 10 mL of freshly distilled toluene. In another Schlenk tube 1 equiv of **2** (0.33 mmol, 0.206 g) was dissolved in 10 mL of freshly distilled toluene and added slowly to **1** within 30 min using a stainless steel cannula. The yellow mixture was warmed slowly and refluxed for 16 h. Subsequent removal of the solvent and drying at 90 °C under vacuum (10^{-3} mbar) yielded an orange solid sublimed at the glass wall of the Schlenk tube. **3** shows decomposition at 292 °C. Anal. Calcd for $\text{C}_{16}\text{H}_{28}\text{CeNSi}_2$: C, 44.6; H, 6.6; Ce, 32.5; N, 3.3. Found: C, 45.2; H, 6.3; Ce, 31.9; N, 3.0. IR (KBr): 3081 m, 2952 m, 2894 w, 2706 w, 2410 m, 2142 w, 1672 w, 1536 w, 1437 m, 1413 sh, 1356 w, 1248 m, 1241 m, 1183 w, 1033 m, 1011 s, 935 w, 867 m, 839 m, 823 m, 810 s, 767 s, 786 s, 675 w, 594 m cm^{-1} . EI-MS:

(38) Bradley, D. C.; Ghotra, J. S. *Inorg. Chim. Acta* **1975**, *13*, 11.

(39) Hou, Z.; Wakatsuki, Y. *Sci. Synth.* **2003**, *2*, 849.

(40) Lappert, M. F.; Singh, A. *Inorg. Synth.* **1990**, *27*, 168.

(41) Brauer, G. In *Handbuch der präparativen anorganischen Chemie*, 3rd ed.; Ferdinand Enke: Stuttgart, Germany, 1975; Vol. 1, p 444.

(42) Krauss, H. L.; Stach, H. *Z. Anorg. Allg. Chem.* **1969**, *366*, 34.

m/z 429 (5, M – H), 359 (70, Cp₂CeNH(SiMe₃)), 345 (15, Cp₂CeNH(SiMe₂)), 331 (20, Cp₂CeNH(SiMe)), 293.8 (100, CpCeNH(SiMe₃)), 279 (15, CpCeNH(SiMe₂)), 270 (Cp₂Ce), 75 (SiMe₃), 66 (Cp).

X-ray Crystallography. Since reflection data were collected with different instruments, data reduction was performed with different program packages. For Cp₃Ce the STOE IPDS software package was used, and for Cp₃Ho the Bruker Collect program package (scalepack cell, hkl scalepack and hkl Denzo) was used. Subsequent calculations after the determination of the unit-cell parameters and data reduction to the hkl format were carried out using the SHELXS⁴³ and SHELXL⁴⁴ programs. Analytical scattering factors for neutral atoms were used throughout the analysis. Hydrogen atoms were either treated isotropically, if found in the Fourier maps, or were otherwise included manually using a riding model.

Powder reflection data were collected with a STOE Stadi P powder diffractometer (Cu K α_1 radiation) in Debye–Scherrer geometry. The single-phase samples were sealed in 0.2–0.3 mm capillaries under an argon atmosphere. For the unit cell refinement of Cp₃Ce, Cp₃Dy, and Cp₃Ho the cell constants and atom positions were obtained by single-crystal measurements of these compounds. Cell refinements (LeBail profile fitting, Rietfeld method) were carried out with the GSAS program package.⁴⁵

MAS NMR Experiments. The ¹H MAS NMR and ¹³C{¹H} RAMP CP MAS NMR experiments were carried out on a Bruker Avance DSX spectrometer equipped with a commercial 2.5 mm MAS NMR double-resonance probe. The magnetic field strength was 11.75 T, corresponding to a ¹³C resonance frequency of 125.8 MHz. All spectra were acquired using a continuous-wave decoupling of approximately 110 kHz ¹H decoupling field strength. A commercially available pneumatic control unit was used to limit

MAS frequency variations to a 2 Hz interval for the duration of the experiment. Samples were spun at 4 kHz. The chemical shift values given refer to tetramethylsilane (TMS) as the external chemical shift reference. The chemical shift values refer to a deshielding scale. The repetition rate of the experiments is 3 s. Typically 96 transients per ¹³C spectrum were accumulated. Simulations of the chemical shift parameters were done by minimizing the squared difference between experiment and simulation using the SIMPSON MINUIT routines⁴⁶ and the same chemical shift conventions as in SIMPSON.⁴⁷

Acknowledgment. We are indebted to the following people for conducting the physical measurements: Dr. Peter Mayer (single crystal X-ray diffractometry), Dagmar Ewald and Dr. Gerd Fischer (mass spectrometry), Bettina Lotsch (low temperature X-ray powder diffractometry) (all Department Chemie und Biochemie, Universität München (LMU)). Financial support by the Deutsche Forschungsgemeinschaft (DFG) (Schwerpunktprogramm SPP 1166, Lanthanoidspezifische Funktionalitäten in Molekül und Material, project SCHN377/10), the Fonds der Chemischen Industrie, and the Emmy-Noether Programm (DFG) is also gratefully acknowledged.

Supporting Information Available: Crystallographic data for Cp₃Ho and Cp₃Ce as CIF files. This material is available free of charge via the Internet at <http://pubs.acs.org>. These data have also been deposited with the Cambridge Crystallographic Data Centre; copies of the data CCDC 600221–600223 can be obtained free of charge by www.ccdc.cam.ac.uk/data_request/cif, by emailing data_request@ccdc.cam.ac.uk, or by contacting The Cambridge Crystallographic Data Centre, 12, Union Road, Cambridge CB2 1EZ, U.K. (fax +44 1223 336033).

OM060226W

(43) Sheldrick, G. M. SHELXS-97; University of Göttingen, Göttingen, Germany, 1997.

(44) Sheldrick, G. M. SHELXL-97; University of Göttingen, Göttingen, Germany, 1997.

(45) von Dreele, R. B.; Larson, A. C. *Los Alamos Natl. Lab., Rep.* **1990**, LAUR 86-748.

(46) Vosegaard, T.; Malmendal, A.; Nielsen, N. C. *Monatsh. Chem.* **2002**, *133*, 1555.

(47) Bak, M.; Rasmussen, J. T.; Nielsen, N. C. *J. Magn. Reson.* **2000**, *147*, 296.